

# Temperature Evolution of the Diffusive Dynamics of Disaccharide Aqueous Solutions by Quasielastic Neutron Scattering

C. Branca,<sup>†</sup> S. Magazù,<sup>\*,†</sup> G. Maisano,<sup>†</sup> and M. T. F. Telling<sup>‡</sup>

Dipartimento di Fisica dell'Università di Messina and INFM, 98166 Messina, Italy, and ISIS Pulsed Neutron Facility, Rutheford Appleton Laboratory, Chilton, Didcot, Oxon, OX1 10QX, United Kingdom

Received: April 26, 2004; In Final Form: July 5, 2004

To investigate the dynamics of homologous disaccharide aqueous solutions, quasielastic neutron scattering (QENS) measurements were performed on trehalose and sucrose aqueous solutions at different temperatures. Neutron spectra were collected by using the spectrometer OSIRIS at the ISIS pulsed neutron source of the Rutheford Appleton Laboratory (Chilton, U.K.). The employment of H/D substitution allowed the separation of the diffusive dynamics of water from that of the disaccharide. The analysis of the trehalose transport properties suggests the existence of a transition between a hopping mechanism of the sugar molecules trapped inside cages formed by neighboring molecules, and a continuous diffusion. Moreover, the presence of disaccharides markedly influences, over all of the temperature range investigated, the dynamics of the hydration water determining a slowing down in comparison with the bulk water. This results in a more pronounced effect for the trehalose/H<sub>2</sub>O solution than for the sucrose one, so confirming previous QENS and NMR results.

## 1. Introduction

Among different methodologies available in the field of preservation of high added value products, the use of natural bioprotectors, such as disaccharides, and trehalose above all, is worthy of mention. The interest in trehalose is due to its extraordinary effectiveness as a bioprotector in dehydration and freezing processes.<sup>1–3</sup> It is well-known, in fact, that cells degrade if the water content falls below the critical value of 20–30%, unless they are able to maintain intact the native conformation necessary for cellular functions. This is the case for some organisms, such as cryptobiontes, that, thanks to the synthesis of trehalose, are able to survive in a dormant state in dry conditions and then to “resuscitate” when environmental humidity permeates the cell, restoring the original conditions; this state can also be induced in nonadapted cells through the addition of exogenous trehalose. Trehalose is also commonly found in spores, in yeasts, and in the cysts of *Artemia salina*.<sup>4–6</sup> It has also been found that disaccharides accumulate in seaweeds, in lichens, and in some prokaryotes such as *Pseudomonas aeruginosa*, *Escherichia coli*, etc.<sup>5,6</sup> Disaccharides are also found to be effective cryoprotectors as they are able to maintain intact the membrane structure both at high and low temperatures.<sup>7–11</sup>

In view of the increasing interest toward the industrial exploitations of disaccharide-based bioprotectors, in past years disaccharide/water systems have been studied to analyze some of the structural and dynamical properties<sup>12–21</sup> as well as the thermoprotective and thermoactivation action of sugar on enzymes,<sup>22</sup> liposomes,<sup>23</sup> and isolated biological membranes or proteins.<sup>13,22–24</sup>

Up to now, different hypotheses for bioprotection have been formulated,<sup>6–11</sup> but none can be considered fully satisfactory. Evidently the bioprotective effectiveness of disaccharides reflects a complex array of interactions at the structural, physiological,

and molecular levels. However, even if many of the mechanisms remain cryptic, it is clear that they involve interactions that derive from the unique properties of the water molecules.

In our previous Raman<sup>17,18</sup> and INS<sup>20</sup> works, it has been shown that, among disaccharides, trehalose has the greatest destructuring effect on the tetrahedral hydrogen bonded network of water. As a result, the amount of freezable water is reduced and the crystallization process obstructed. The different rigidity of both trehalose/H<sub>2</sub>O and sucrose/H<sub>2</sub>O mixtures has been also characterized by means of neutron scattering measurements,<sup>19</sup> providing information on the low-frequency dynamics and on the thermal mean square atomic fluctuations through the temperature behavior of the Debye–Waller factor. According to this study, the trehalose/H<sub>2</sub>O system plays the role, in comparison with sucrose/H<sub>2</sub>O, of the strongest system.

Besides the influence of disaccharides on the structural properties of water, the changes induced by the presence of disaccharides on the dynamical properties of water have been extensively investigated.

Simulation studies performed by Grigeira et al.<sup>9</sup> seemed to support the hypothesis that the bioprotectant effectiveness is not related to the modification of the peculiarities of water molecules. In particular, by adopting an SPC/E model and some particular initial conditions, these authors concluded that the water dynamics is not affected by the presence of the disaccharide and that the spacing between the idroxyl groups of trehalose perfectly matches the positions of the oxygens in the tetrahedral network of water. In such a way they support the “water-replacement hypothesis” by Crowe et al.,<sup>13</sup> since they relate the bioprotective effectiveness to the ability of trehalose to substitute some water molecules bonded to the biological structures.

Contrary to this hypothesis, different molecular dynamics (MD) studies<sup>25,26</sup> on carbohydrates in solution showed that the water self-diffusion coefficient around the whole trehalose and around its oxygen atoms is strongly modified, being around 25% smaller than in pure water. Moreover, a recent comparative MD

\* Corresponding author. E-mail: fisica@iol.it.

<sup>†</sup> Università di Messina and INFM.

<sup>‡</sup> Rutheford Appleton Laboratory.

study on trehalose, sucrose, and maltose in water solutions, at different concentrations and temperatures, showed that trehalose is the most effective in slowing down the water dynamics, inducing a more extensive hydration layer. This latter result is supported by a preliminary QENS experiment,<sup>21</sup> which suggests that trehalose, at a fixed temperature, affects significantly the dynamics of water molecules in its neighborhood consistently with the presence of a series of hydration layers or shells each of which is characterized by a relatively slow diffusion.

The main purpose of the present work is to obtain relevant information, over a wide temperature range, on the dynamical properties of trehalose/water solution and to compare them with those of sucrose. To this purpose, QENS measurements on trehalose and sucrose both in D<sub>2</sub>O and H<sub>2</sub>O have been performed. From the data analysis the transport properties of both sugar and hydration water have been determined, so providing useful information in the development of theories of bioprotection.

## 2. Experiment

Aqueous solutions of ultrapure  $\alpha,\alpha$ -trehalose and sucrose, purchased by Aldrich-Chemie, were investigated at a molar fraction  $\phi = 0.05$ ,  $\phi = n_d/(n_d + n_w)$ ,  $n_d$  and  $n_w$  being the solute and water mole numbers, respectively. The solutions were prepared by using double distilled and deionized water and heavy water. Measurements were performed on trehalose solutions at different temperatures between 283 and 343 K and, for comparison, on sucrose solutions at  $T = 303$  K.

The QENS experiment was carried out using the OSIRIS inverted geometry spectrometer at the ISIS facility at the Rutherford Appleton Laboratory (Chilton, U.K.). The sample was contained in an aluminum cell with thicknesses 0.3 and 1 mm for H<sub>2</sub>O and D<sub>2</sub>O solutions, respectively. The quasi/inelastic setting consists of a PG002 analyzer that covers a  $Q, \omega$ -domain extending from 0.24 and 1.38 Å<sup>-1</sup> (momentum transfer) and  $-0.5 < \Delta E < 0.5$  meV (energy transfer). The mean energy resolution was  $\Gamma = 24.5$   $\mu$ eV of full width at half-maximum (fwhm), as determined by reference to a standard vanadium plate. Such an energy resolution allows one to observe motions faster than approximately  $2\pi\hbar/\Gamma \approx 170$  ps.

The data were corrected to take into account incident flux, cell scattering, self-shielding, and detector response. Since an average transmission of 90% was calculated for the hydrogenated samples, multiple scattering corrections were neglected.

As with all H<sub>2</sub>O-hydrated hydrocarbons, the ratio of protons to other nuclei is larger than 1. Therefore the spectra measured are essentially due to incoherent scattering from the protons. The calculated total bound scattering cross-section of C<sub>12</sub>H<sub>22</sub>O<sub>11</sub>·19H<sub>2</sub>O is 5.09 kbarn (1 kbarn (1 kb) = 10<sup>-21</sup> cm<sup>2</sup>); 0.30 kb of this value is due to coherent scattering so that the contribution of the latter to the total cross-section amounts to nearly 6%. For the deuterated solutions, the contribution of the coherent scattering to the total cross-section amounts to nearly 20%.

**Method of Data Analysis.** In a QENS experiment the measured quantity is the dynamic structure factor  $S(Q, \omega)$  measured as the distribution of neutrons have undergone an energy exchange,  $\hbar\omega$ , and a momentum change,  $Q$ , after scattering by the sample.<sup>27–29</sup> The intensity of the scattered neutrons splits into two contributions: the “coherent” and “incoherent” scattering. In the case of the hydrogenated solutions, the coherent contribution, as stressed above, can be neglected entirely. In the case of the deuterated solutions the detected signal can be also considered as incoherent to a very good approximation. In such a way, for both the deuterated and

hydrogenated solutions we are mainly concentrating on only one term, that is, the incoherent dynamical structure factor,  $S_{\text{inc}}(Q, \omega)$ .

Assuming that the different kinds of motions in disaccharide water mixtures are not coupled to each other, and following the procedure reported in ref 21, we describe the translational motion in terms of a single Lorentzian, where  $\Gamma_1$  is the half-width at half-maximum (HWHM):

$$S_{\text{trans}}(Q, \omega) = \frac{1}{\pi} \frac{\Gamma_1(Q)}{\Gamma_1^2(Q) + \omega^2} \quad (1)$$

By assuming the series for the rotational model is arrested to the first term,<sup>28</sup> the total incoherent dynamical structure factor we adopted to describe the disaccharide dynamics in D<sub>2</sub>O is the following:

$$S_{\text{inc}}(Q, \omega) = A_0(Q) \left[ F(Q) \frac{1}{\pi} \frac{\Gamma_1(Q)}{\Gamma_1^2(Q) + \omega^2} + (1 - F(Q)) \frac{1}{\pi} \frac{\Gamma_2(Q)}{\Gamma_2^2(Q) + \omega^2} \right] \otimes \text{Res}(Q, \omega) \quad (2)$$

where  $A_0(Q)$  is the Debye–Waller factor,  $F(Q)$  is the elastic incoherent scattering factor (EISF),  $\Gamma_2$  the HWHM of the Lorentzian describing the rotational motion, and  $\text{Res}(Q, \omega)$  is the experimentally determined resolution function.

As far as the hydrogenated samples are concerned, the water contribution to the measured intensity must be included. Ultrasonic velocity measurements indicate that the hydration number for the investigated disaccharides are between 9 and 12 in the temperature range between 343 and 283 K. Therefore, we can assume the water molecules present in our mixtures are very close to the solute so that no bulk water contribution is present. Starting from these considerations, the resulting scattering law observed in the experiment is a linear combination of two terms:

$$S_{\text{inc}}(Q, \omega) = \frac{2}{\hbar} [f_{\text{disacch}} S_{\text{disacch}}(Q, \omega) + f_{\text{hyd}} S_{\text{hyd}}(Q, \omega)] \quad (3)$$

where  $S_{\text{disacch}}(Q, \omega)$ , and  $S_{\text{hyd}}(Q, \omega)$  are the dynamical structure factors of the hydrated disaccharide (disaccharide and its first hydration shell) and of the hydration water (water molecules in the second, third hydration shells), respectively.  $f_{\text{disacch}}$  and  $f_{\text{hyd}}$  represent fraction factors of the total scattering from disaccharides and their strongly bonded water molecules and from hydration water, respectively: the relation  $f_{\text{disacch}} + f_{\text{hyd}} = 1$  must be fulfilled. The dynamics of the hydration water has been analyzed in terms of a third Lorentzian component with a HWHM  $\Gamma_3$ . Even if the inclusion of a term describing the rotational diffusion of the mobile water fraction is in principle possible, such an analysis does not improve the fit quality.

The whole scattering function for the hydrogenated samples results:

$$S_{\text{inc}}(Q, \omega) = e^{-\langle u^2 \rangle Q^2/3} \left\{ f_{\text{disacch}} \left[ F(Q) \frac{1}{\pi} \frac{\Gamma_1(Q)}{\Gamma_1^2(Q) + \omega^2} + (1 - F(Q)) \frac{1}{\pi} \frac{\Gamma_2(Q)}{\Gamma_2^2(Q) + \omega^2} \right] + f_{\text{hyd}} \frac{1}{\pi} \frac{\Gamma_3(Q)}{\Gamma_3^2(Q) + \omega^2} \right\} \quad (4)$$

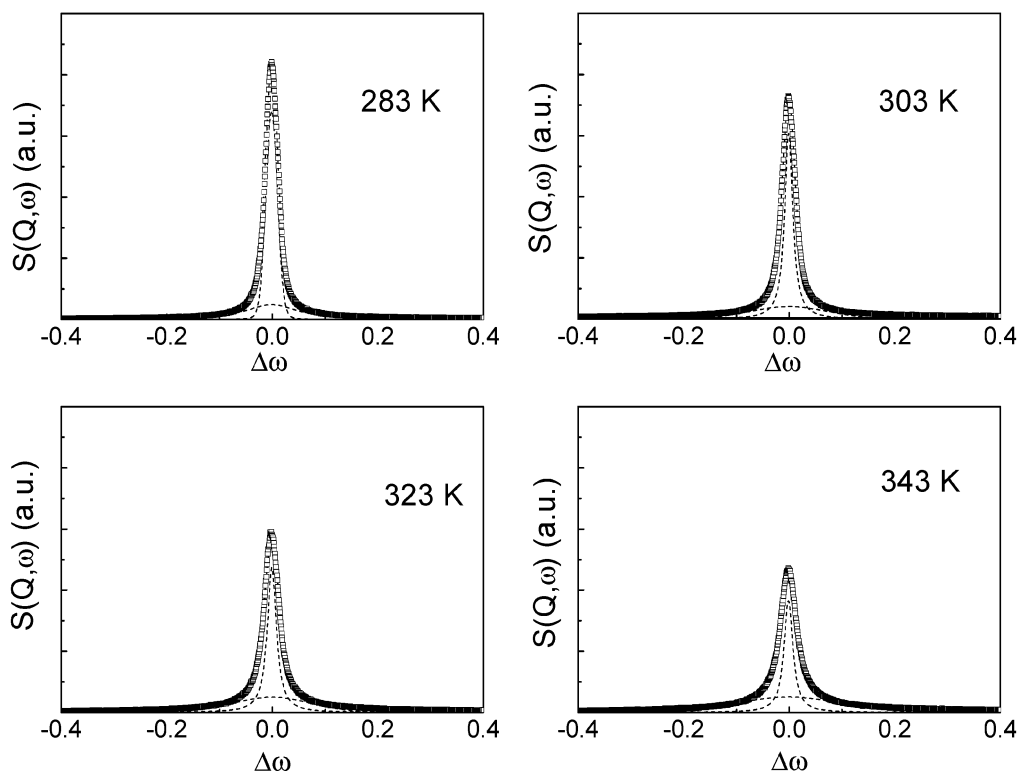


**Figure 1.** Normalized QENS spectra of trehalose/D<sub>2</sub>O at different temperatures at  $Q = 1.12 \text{ \AA}^{-1}$ . The continuous line is the fit result obtained by using relation 2; the dashed lines refer to the Lorentzian components.

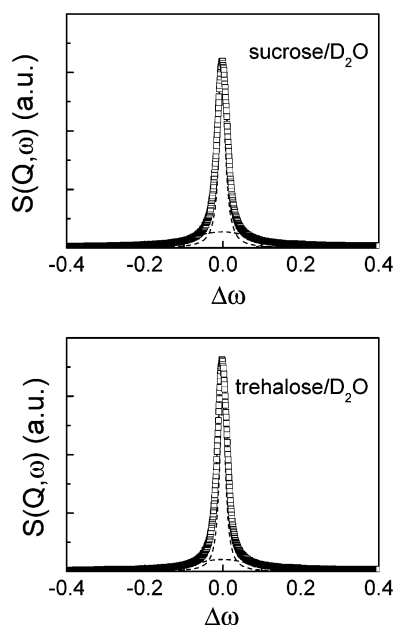


**Figure 2.** QENS spectra of sucrose/D<sub>2</sub>O and trehalose/D<sub>2</sub>O,  $Q = 1.12 \text{ \AA}^{-1}$ , at  $T = 303 \text{ K}$ . The continuous line is the fit result obtained by using relation 2; the dashed lines refer to the Lorentzian components.

$\Gamma_1$ ,  $\Gamma_2$ , and  $F(Q)$  are the same for both the deuterated and hydrogenated spectra.

### 3. Results and Discussion

Figure 1 shows, as an example, the normalized QENS spectra at  $Q = 1.12 \text{ \AA}^{-1}$  for the trehalose/D<sub>2</sub>O solutions,  $\phi = 0.05$ , at different temperatures, together with the fit components according to relation 2. In Figure 2 a comparison of the QENS spectra, together with the fitting components, for the trehalose- and sucrose/D<sub>2</sub>O solutions at the same molar fraction,  $\phi = 0.05$ ,

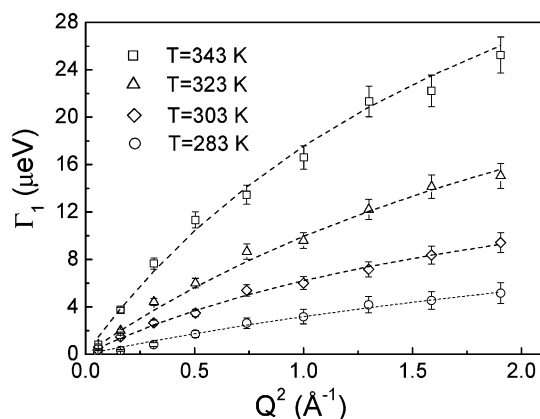


**Figure 3.**  $Q^2$ -dependence of the translational component ( $\Gamma_1$ ) half-width at half-maximum for trehalose at different temperatures. The lines are the best fit according to the RJD model.

at  $T = 303 \text{ K}$  and  $Q = 1.12 \text{ \AA}^{-1}$  is shown. As can be seen, the model gives excellent fits for all the spectra over the entire  $\omega$  range.

From the fitting procedure, the free parameters  $\Gamma_1$ ,  $\Gamma_2$ , and the EISF have been determined. Figure 3 reports the  $\Gamma_1$  values, corresponding to the translational contribution, as a function of  $Q^2$  for the trehalose/D<sub>2</sub>O solution at different temperatures. As is well-known, continuous diffusion predicts QENS line widths to increase linearly as  $Q^2$ . In our case, this holds true for the lowest  $Q$  values, but for larger  $Q$  the widths clearly bend downward versus  $Q^2$ . Starting from this observation, we have chosen to describe the  $\Gamma_1(Q)$  variation by the random jump diffusion (RJD) model,<sup>29</sup> even if a saturation of the  $\Gamma_1$  values at high  $Q$  values is not displayed especially at the highest temperature. This can be due to both the limited  $Q$  range investigated and, as we will see in the following, the possible change in the diffusion mechanisms at temperatures higher than

**TABLE 1: Self-Diffusion Coefficients,  $D_s$ , Residence Times,  $\tau_0$ , and Mean Square Jump Lengths,  $\langle l^2 \rangle_{av}^{1/2}$ , for Trehalose- and Sucrose/D<sub>2</sub>O Solutions at Different Temperatures**

$T$ (K)	$D_s \times 10^{-6}$ (cm <sup>2</sup> /s)	$\tau_0$ (ps)	$\langle l^2 \rangle_{av}^{1/2}$ (Å)
Trehalose/D <sub>2</sub> O			
283	0.61	49.20	1.33
303	1.07	25.48	1.27
323	1.55	12.91	1.09
343	3.05	5.48	1.00
Sucrose/D <sub>2</sub> O			
303	1.60	33.00	1.78

those investigated here. In the frame of the RJD model the  $\Gamma_1(Q)$  is described by

$$\Gamma_1(Q) = D_s Q^2 / (1 + D_s Q^2 \tau_0) \quad (5)$$

where  $\tau_0$  represents the residence time and  $D_s$  the translational diffusion constant. The dashed lines in Figure 3 represent the best fit according to this model. The  $D_s$  and  $\tau_0$  values obtained from the fit procedure for the trehalose- and sucrose/D<sub>2</sub>O mixtures are reported in Table 1. In the same table, the mean square jump lengths  $\langle l^2 \rangle_{av}^{1/2}$ , given in terms of the translational diffusion coefficient by  $\langle l^2 \rangle_{av} = 6D_s\tau_0$ , are also reported. The obtained fitting parameters are well-comparable with previous QENS<sup>21</sup> results on trehalose/D<sub>2</sub>O solution at the same concentration at  $T = 323$  K obtained by using the IRIS spectrometer ( $D_s = 1.63 \times 10^{-6}$  cm<sup>2</sup>/s;  $\tau_0 = 13.3$ ;  $\langle l^2 \rangle_{av}^{1/2} = 1.3$  Å). Similar  $D_s$  values have been also obtained by NMR<sup>30–32</sup> even if a direct comparison is only possible for similar techniques. However the activation energy value for the trehalose/D<sub>2</sub>O mixture,  $E_a = 6$  kcal/mol, obtained by fitting the  $D_s$  values to the Arrhenius law (see Figure 4) is comparable with that derived from NMR<sup>31,32</sup> on the same system at the same concentration ( $E_a = 6.5$  kcal/mol). Moreover, both QENS and NMR measurements evidence a slower diffusion for trehalose in comparison with sucrose. This can be partly attributed to the smaller hydration number of sucrose as inferred by previous density and ultrasonic velocity findings.<sup>33,34</sup>

As can be seen from Table 1 and Figure 4, the trehalose mobility increases with increasing temperature from 283 to 343 K. In the same temperature range, a strong decreasing of the jump time from around 49 to 5 ps and a corresponding variation of the mean jump lengths are also observed. Starting from these observations one can hypothesize not only a slowing down of the trehalose mobility with decreasing temperature but also a variation in the geometry of motion. To better evidence this feature we analyze the temperature behavior of the EISF parameter, the  $Q$  dependence of which is reported in Figure 5 for different temperatures.

As can be seen, the EISF values do not approach zero in the investigated  $Q$  range and are strongly temperature-dependent, indicating that the volume accessible to the scatterers varies when the temperature is changed. In principle, by analyzing  $F(Q)$ , we should be able to distinguish between several types of motion even if, since we only observe an average of all types of motions, the variation of  $F(Q)$  with  $Q$  may only give very rough information on the shape of the motion. Keeping in mind this consideration, different models proposed in the literature have been taken into consideration. The most reliable among them, assumes the EISF is composed of a constant term, particularly significant at the lowest temperatures, arising from the hydrogen atoms that do not diffuse on the time scale of the experimental resolution and of a  $Q$ -dependent term arising from the mobile hydrogen atoms. With reference to this  $Q$ -dependent term, the best parametric statistics have been obtained by fitting

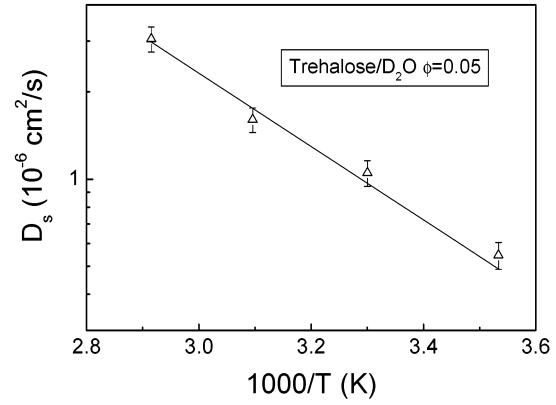


**Figure 4.** Arrhenius plot of the diffusion coefficient values for the trehalose/D<sub>2</sub>O mixture. The solid line is the fit result to the Arrhenius law.

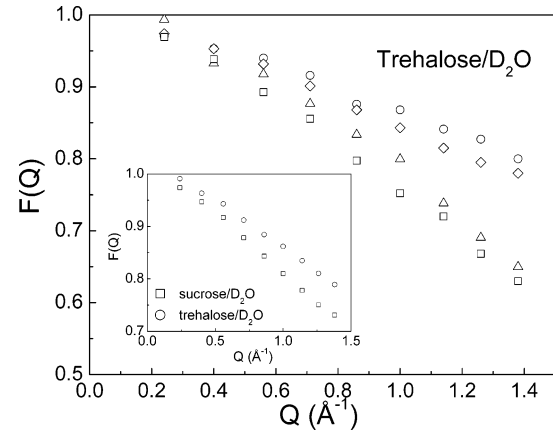


**Figure 5.**  $Q$ -dependence of the EISF parameter at different temperatures for the trehalose/D<sub>2</sub>O mixture (up triangles,  $T = 283$  K; circles,  $T = 303$  K; down triangles,  $T = 323$  K; squares,  $T = 343$  K). In the insert, a comparison of the EISF values for trehalose- and sucrose/D<sub>2</sub>O mixtures, at  $T = 303$  K, is reported.

the data according to the two-site jump model which assumes  $F(Q) = 0.5[1 + j_0(Qd)]$ ,  $j_0(x)$  being the zero-order Bessel spherical function of the first kind and  $d$  the jump distance between the two sites. By adopting this model, we obtain, at the different temperatures investigated,  $d$  values ranging between 1 and 1.5 Å. These values are in good agreement with the mean jump length values, but not compatible with the radius of the hydrated disaccharides ( $\sim 6$  Å). We can therefore assume that the sugar molecules, trapped inside cages created by the surrounding molecules, are not able to fully rotate, especially at the lowest temperatures, but rather undergo random jumps followed by highly damped motions, such as hindered rotations. However, as suggested by the drastic change in the slope of the  $F(Q)$  above 303 K a change in the mechanisms of motion occurs with increasing temperature. In fact as suggested, by the decreasing values of  $\langle l^2 \rangle_{av}^{1/2}$ , as well as by the large decrease in time between jumps, it is possible to hypothesize the existence of a transition, above room temperature, between a hopping mechanism and a continuous diffusion inside volumes more and more large that, however, would be completely set in at temperatures higher than those investigated in the present work. This is also confirmed by the increased rotational mobility of trehalose as the temperature increases ( $\langle \Gamma_2 \rangle \approx 60, 75, 85$ , and  $105 \mu\text{eV}$  at  $T = 283, 303, 323$ , and  $343$  K, respectively). This interpretation is supported by previous experimental<sup>35,36</sup> and simulation work<sup>32,37</sup> on different mono- and disaccharides, according to which the mechanisms of diffusion of the sugar



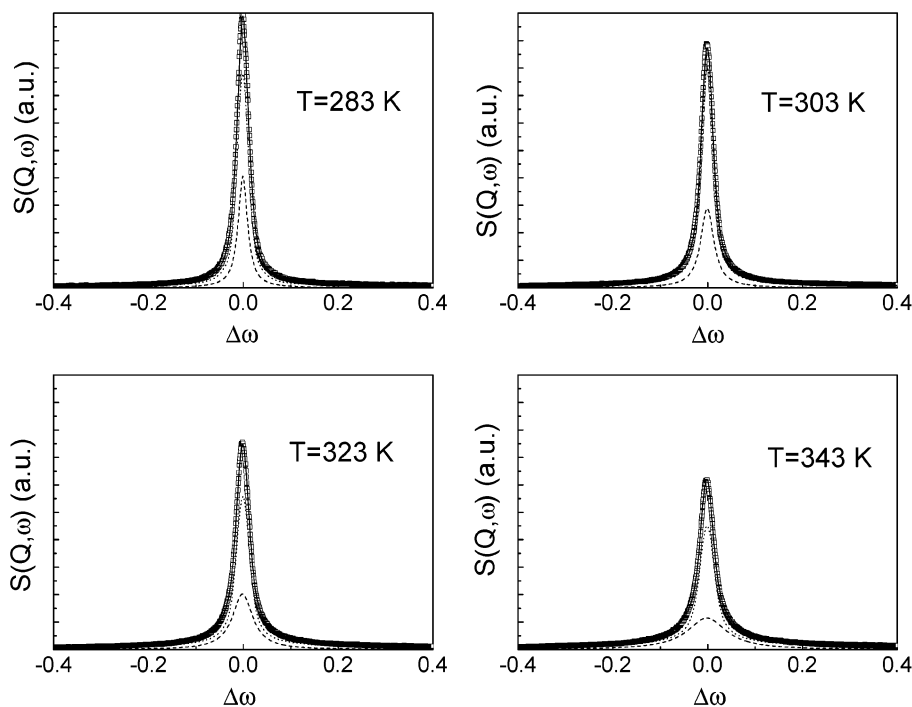


**Figure 6.** Normalized QENS spectra for the trehalose/H<sub>2</sub>O sample at different temperatures. Squares, experimental data; continuous line, fit according to relation 4; dotted lines, trehalose component; dashed lines, water component.

molecules varies significantly as the temperature is decreased or the concentration increased.

The sudden change in the mobility of the system above 303 K is also confirmed by the decreasing of the percentage of “immobile” hydrogens, obtained by the plateau value of the EISF, as the temperature increases. This results in being nearly 78% of the total up to 303 K, whereas, at higher temperatures, this percentage decreases to  $\sim 60\%$ . Finally, by comparing the EISF parameter for trehalose- and sucrose/D<sub>2</sub>O mixtures at the same temperature (see the insert of Figure 5), we observe a higher percentage of “immobile” hydrogens for the trehalose/D<sub>2</sub>O mixture in comparison with the sucrose one. This result, together with the lower value for the jump distance,  $d$ , outlines a picture according to which the sucrose/D<sub>2</sub>O system appears to be more flexible than the trehalose one, so supporting previous neutron scattering findings.<sup>19</sup>

We now consider the results obtained for the hydrogenated solutions analyzed in terms of relation 4. As an example, in Figure 6, the normalized QENS spectra for the trehalose/H<sub>2</sub>O samples at different temperatures are reported together with the fitting components.

In Figure 7 the  $Q^2$  dependence of the water component ( $\Gamma_3$ ) HWHM is reported. Once more, the data have been fitted according to the RJD model. The fit parameters, that is, the self-diffusion coefficients,  $D_w$ , the residence times,  $\tau_1$ , and the mean jump lengths are reported in Table 2. As can be seen,  $\langle l^2 \rangle_{av}^{1/2}$  are temperature-dependent, being smaller at higher temperatures. This can be interpreted in terms of the network model for the disaccharide/H<sub>2</sub>O systems. Previous experimental<sup>17,18,20</sup> and simulation<sup>26</sup> works showed that the presence of disaccharides modifies the tetrahedral hydrogen bonded network of pure water and that this effect is, on average, more marked at higher temperatures.<sup>38</sup> It is therefore reasonable obtaining, above room temperature,  $\langle l^2 \rangle_{av}^{1/2}$  values smaller than the distance across the tetrahedral angle in pure water, which is equal to 1.6 Å,<sup>39</sup> that decrease by increasing temperature when the distribution of hydrogen bonds is more deformed. Moreover, since, among homologous disaccharides, trehalose has, at a fixed

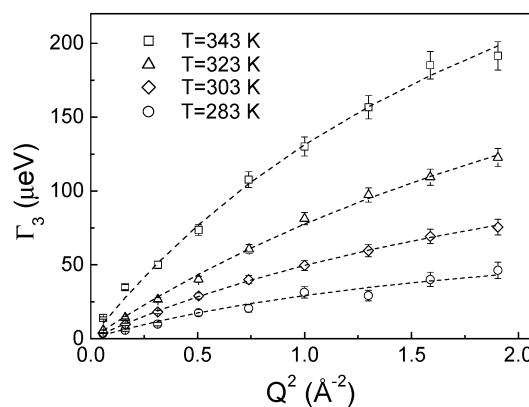


**Figure 7.**  $Q^2$ -dependence of the water component ( $\Gamma_3$ ) half-width at half-maximum for the trehalose/H<sub>2</sub>O sample at different temperatures. The lines are the fit results according to the RJD model.

**TABLE 2: Self-Diffusion Coefficients,  $D_w$ , Residence Times,  $\tau_1$ , and Mean Square Jump Lengths,  $\langle l^2 \rangle_{av}^{1/2}$ , for Water in Trehalose and Sucrose Solutions at Different Temperatures**

$T$ (K)	$D_w \times 10^{-5}$ (cm <sup>2</sup> /s)	$\tau_1$ (ps)	$\langle l^2 \rangle_{av}^{1/2}$ (Å)
Trehalose/H <sub>2</sub> O			
283	0.65	7.26	1.63
303	1.00	3.05	1.35
323	1.48	1.76	1.25
343	2.49	0.99	1.21
Sucrose/H <sub>2</sub> O			
303	1.15	2.85	1.40

temperature, the greatest destructuring effect on the tetrahedral hydrogen bonded network of water,<sup>18,20</sup> the lower  $\langle l^2 \rangle_{av}^{1/2}$  value observed for the trehalose/H<sub>2</sub>O solution, in comparison with the sucrose one at  $T = 303$  K, can be justified.

Finally, to check the influence of disaccharides into the water dynamics, we analyzed the temperature dependence of the self-diffusion coefficients for the hydration water,  $D_w$ , reported in Figure 8 together with the values obtained from NMR measurements.<sup>31,32</sup> For comparison the diffusion coefficients for pure

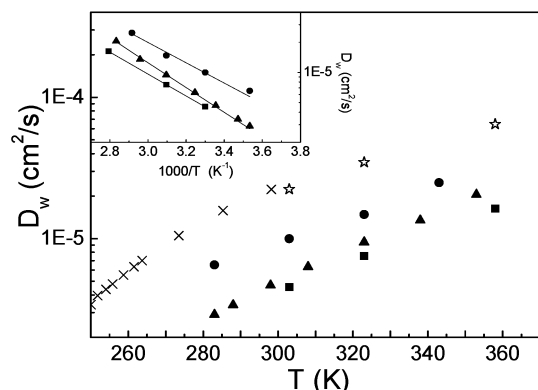


**Figure 8.** Diffusion coefficients for pure water and for water in trehalose solution,  $\phi = 0.05$ . The values for water come from ref 40 (crosses) and from ref 32 (stars). Data for trehalose come from the present study (circles) and from NMR measurements (refs 31 and 32, triangles and squares, respectively). In the insert the corresponding Arrhenius plot of the diffusion coefficient values for the trehalose/ $\text{H}_2\text{O}$  mixture is reported. The solid lines are the fit results to the Arrhenius law.

water<sup>32,40</sup> are also reported. Notwithstanding the QENS values do not coincide with the NMR data, these latter being slightly lower, it is interesting observing that both QENS and NMR data evidence a slowing down of the hydration water's translational motion in the presence of disaccharides in comparison with bulk water and a faster water dynamics in the presence of sucrose than in the presence of trehalose. A similar slowing down of the dynamics of the hydration water has been also observed in monosaccharide solutions.<sup>35,36,41</sup> Moreover, the activation energy value we obtained ( $E_a = 4.7$  kcal/mol) is comparable to the values derived from NMR measurements ( $E_a \approx 5 \div 5.6$  kcal/mol).<sup>31,32</sup>

Finally, it is interesting to compare the activation energy for the trehalose/water solution with that for glucose obtained by previous QENS findings.<sup>41</sup> Since trehalose is a disaccharide of glucose, one should expect for the trehalose/ $\text{H}_2\text{O}$  solution an activation energy twice as much as that for glucose at the same concentration. Indeed, if we compare the activation energies for the two solutions at a concentration  $\phi = 0.05$ , we observe that trehalose has an activation energy only 1.2 times higher than that of glucose ( $E_a = 3.8$  kcal/mol). In our opinion this is due to the different hydration number of the two sugars that is to the different number of water molecules tightly bonded to the sugar ( $n_H \approx 12$  for trehalose and  $n_H \approx 5$  for glucose<sup>42</sup>). In fact, if we compare the activation energies for two solutions of trehalose and glucose characterized by the same ratio between bound and free water molecules (for example the trehalose/water solution at  $\phi = 0.05$  with the glucose/water solution at  $\phi = 0.09$ ), we obtain comparable values ( $E_a \approx 4.8$  kcal/mol<sup>41</sup>).

#### 4. Conclusions

To investigate the diffusive behavior of trehalose at different temperatures and to compare the diffusive dynamics of homologous disaccharides, quasielastic neutron scattering data for sucrose- and trehalose/water mixtures at different temperatures have been analyzed. The employment of H/D substitution allowed the separation of the diffusive dynamics of water from that of the disaccharide.

For what concerns the trehalose dynamics, the analysis of the data has evidenced a transition, with increasing temperature from 283 to 343 K, between a hopping mechanism between cages formed by neighboring molecules, and a continuous

diffusion that, however, would be completely set in at temperatures higher than those investigated in the present work. Moreover, it has been possible evidencing a higher mobility for sucrose than for trehalose probably due to the smaller hydration number of sucrose.

The analysis of the hydrogenated samples has shown that the presence of disaccharides markedly influences, over all the temperature range investigated, the dynamics of the hydration water determining a slowing down in comparison with the bulk water. Moreover, this effect is more pronounced in the presence of trehalose than of sucrose, so confirming previous QENS and NMR results.

Finally, the temperature behavior of the mean jump length, interpreted in terms of the network model for the disaccharide/ $\text{H}_2\text{O}$  systems, is perfectly compatible with the proved higher destructuring effectiveness of trehalose on the tetrahedral hydrogen bonded network of pure water. The higher effectiveness in reducing water mobility and in destructuring the tetrahedral hydrogen bonded network of pure water is to be considered, in our opinion, fundamental characteristics in understanding the superior bioprotectant ability of trehalose in comparison with sucrose.

#### References and Notes

- (1) Crowe, J. H.; Crowe, L. M. *Biological Membranes*; Academic Press: New York, 1984; p 57.
- (2) Clegg, J. S. *Comp. Biochem. Physiol.* **1967**, *20*, 8.
- (3) Elbein, A. D. *Chem. Biochem.* **1974**, *30*, 227.
- (4) Vegis, A. *Annu. Rev. Plant Physiol.* **1964**, *15*, 185.
- (5) Sussman, A. S.; Halvorson, H. O. *Spores: Their Dormancy and Germination*; Harper & Row: New York, 1966.
- (6) Crowe, J. H.; Crowe, L. M. *Science* **1984**, *223*, 701.
- (7) Green, J. L.; Angell, C. A. *J. Phys. Chem.* **1989**, *93*, 2880.
- (8) Angell, C. A. *Hydrogen-Bonded Liquids*; NATO-ASI Series, Series B, Vol. 329; Plenum: New York, 1991; p 59.
- (9) Donnamaria, M. C.; Howard, E. I.; Grigera, J. R. *J. Chem. Soc., Faraday Trans.* **1994**, *90*, 2731.
- (10) Leslie, S. B.; Israeli, E.; Lighthart, B.; Crowe, J. H.; Crowe, L. M. *Appl. Environ. Microbiol.* **1995**, *61*, 3592.
- (11) Fox, K. C. *Science* **1995**, *267*, 1922.
- (12) Nwaka, S.; Holzer, H. *Progress in Nucleic Acid Research and Molecular Biology*; Academic Press: New York 1997; p 197.
- (13) Crowe, J. H.; Carpenter, J. F.; Crowe, L. M. *Annu. Rev. Physiol.* **1998**, *60*, 73.
- (14) Crowe, J. H.; Crowe, L. M.; Chapman, D. *Arch. Biochem. Biophys.* **1985**, *236*, 289.
- (15) Magazù, S.; Middendorff, H. D.; Migliardo, P.; Musolino, A. M.; Sciortino, M. T.; Villari, V. *J. Phys. Chem. B* **1998**, *102*, 2060.
- (16) Magazù, S.; Maisano, G.; Migliardo, P.; Middendorff, H. D.; Villari, V. *J. Chem. Phys.* **1998**, *109*, 1170.
- (17) Branca, C.; Magazù, S.; Maisano, G.; Migliardo, P. *J. Phys. Chem. B* **1999**, *103*, 4.
- (18) Branca, C.; Magazù, S.; Maisano, G.; Migliardo, P. *J. Chem. Phys.* **1999**, *111*, 281.
- (19) Branca, C.; Magazù, S.; Maisano, G.; Migliardo, F. *Phys. Rev. B* **2001**, *64*, 224204.
- (20) Branca, C.; Magazù, S.; Maisano, G.; Bennington, S. M.; Fåk, B. *J. Phys. Chem. B* **2003**, *107*, 1444.
- (21) Magazù, S.; Maisano, G.; Migliardo, P.; Villari, V.; Telling, M. T. *F. J. Phys. Chem. B* **2001**, *105*, 1851.
- (22) Carnici, P.; Nishiyama, Y.; Westover, A.; Itoh, M.; Nagaoka, S.; Sasaki, N.; Okazaki, N.; Muramatsu, M.; Hayashizaki, Y. *Biochemistry* **1998**, *95*, 520.
- (23) Sun, W. Q.; Leopold, L. M.; Crowe, L. M.; Crowe, J. H. *Biophys. J.* **1996**, *70*, 1769.
- (24) Hottiger, T.; De Virgilio, C.; Hall, M. N.; Boller, T.; Wiemken, A. *Eur. J. Biochem.* **1994**, *219*, 187.
- (25) Bonanno, G.; Noto, R.; Fornili, S. L. *J. Chem. Soc., Faraday Trans.* **1998**, *94*, 2755.
- (26) Bordat, P.; Lerbret, A.; Demaret, J. P.; Affouard, F.; Descamps, M. *Europhys. Lett.* **2004**, *65*, 41.
- (27) Volino, F.; Dianoux, A. J. *Organic Liquids; Structures Dynamics and Chemical Properties*; Wiley: New York, 1965.
- (28) Volino, F. *Spectroscopic Methods for the Study of Local Dynamics in Polyatomic Fluids*; NATO ASI Series, Series B, Vol. 33; Plenum Press: New York, 1978.

- (29) Bee, M. *Quasielastic Neutron Scattering*; Adam Hilger: Bristol, U.K., and Philadelphia, PA, 1988.
- (30) Branca, C.; Magazù, S.; Maisano, G.; Migliardo, P.; Tettamanti, E. *Physica B* **2000**, *291*, 180.
- (31) Rampp, M.; Buttersack, C.; Lüdemann H. D. *Carbohydr. Res.* **2000**, *328*, 561.
- (32) Ekdawi-Sever, N.; de Pablo, J. J.; Feick, E.; von Meerwall, E. *J. Phys. Chem. A* **2003**, *107*, 936.
- (33) Branca, C.; Magazù, S.; Maisano, G.; Migliardo, F.; Migliardo, P.; Romeo, G. *J. Phys. Chem. B* **2001**, *105*, 10140.
- (34) Branca, C.; Magazù, S.; Maisano, G.; Migliardo, P. *J. Biol. Phys.* **2000**, *26*, 295.
- (35) Smith, L. J.; Price, D. L.; Chowdhuri, Z.; Brady, J. W.; Saboungi, M. L. *J. Chem. Phys.* **2004**, *120*, 327.
- (36) Feeney, M.; Brown, C.; Tsai, A.; Neumann, D.; Debenedetti, P. G. *J. Phys. Chem. B* **2001**, *105*, 7799.
- (37) Roberts, C. J.; Debenedetti, P. G. *J. Phys. Chem. B* **1999**, *103*, 7308.
- (38) Branca, C.; Magazù, S.; Maisano, G.; Bennington, S. M.; Taylor, J. To be submitted for publication.
- (39) Teixeira, J.; Bellissent-Funel, M. C.; Chen, S. H.; Dianoux, A. J. *Phys. Rev. A* **1985**, *31*, 1913.
- (40) Gillen, K. T.; Douglass, D. C.; Hoch, J. R. *J. Chem. Phys.* **1972**, *57*, 5117.
- (41) Talon, C.; Smith, L. J.; Brady, J. W.; Lewis, B. A.; Copley, J. R. D.; Price, D. L.; Saboungi, M. L. *J. Phys. Chem. B* **2004**, *108*, 5120.
- (42) Caffarena, E. R.; Grigera J. R. *Carbohydr. Res.* **1999**, *315*, 63.